



# Photoreductive debromination of decabromodiphenyl ether by pyruvate

Zhaowu Jiang, Wensheng Linghu, Yimin Li, Chunyan Sun\*

Department of Chemistry, Shaoxing University, Shaoxing 312000, Zhejiang, China



## ARTICLE INFO

### Article history:

Received 1 August 2013

Received in revised form

27 December 2013

Accepted 6 January 2014

Available online 28 January 2014

### Keywords:

Polybrominated diphenyl ethers

Pyruvate

Photoreductive

Debromination

## ABSTRACT

Polybrominated diphenyl ethers (PBDEs) have aroused highly environmental concerns because of their toxicity and ubiquitousness in the biological and environmental system. Here, we report that decabromodiphenyl ether (BDE209) undergoes efficient reductive debromination reaction by pyruvate under UV irradiation ( $>360\text{ nm}$ ). The photoreductive degradation kinetics of BDE209 has been further investigated under different reaction conditions. The debromination reactions occur in a stepwise process, producing a series of lower brominated congeners. The debromination shows un conspicuous position-selective property. The possible photoreductive mechanism has been proposed by UV-vis and kinetic isotope effect (KIE). This study not only provides a potential application of removal of PBDEs contaminations but also provides some information for the fate of PBDEs in environment.

© 2014 Elsevier B.V. All rights reserved.

## 1. Introduction

Persistent organic pollutants (POPs) arouse significant scientific concern because they show persistent and bioaccumulative in the environment [1]. Polybrominated diphenyl ethers (PBDEs) have attracted particular attention in this field due to extensive use as flame retardants and global distribution. In recent years, PBDEs have been detected in sediments [2,3], marine organisms [4,5], food samples [6], and human mother's milk [7], even in Arctic animals [8,9]. Some researches indicated that PBDEs accumulated in the body could influence liver enzyme activity and neurological development at a key period of brain growth [10,11].

During the past few years, research on PBDEs has been greatly spread and mighty endeavors have been devoted to study the transformation of PBDEs in the environment. For example, photolytic debromination of PBDEs has been observed on the surface of clay minerals, metal oxides, silica gel, sand, soil and sediment [12,13], and in toluene, hexane or methanol/water [14–16]. The biotic reductive debromination has also been reported by anaerobic bacteria [17], juvenile rainbow trout and common carp [4,5]. Besides the studies on the environmental transformation of PBDEs, the development of potential methods for PBDEs removal in contaminated environmental system is another urgent and significant issue. Zerovalent iron reduction has been proven an effective

method for debromination of PBDEs [18–21]. Photocatalysis has also been studied for degradation of PBDEs [22–25]. For example, BDE209 could be a rapid photocatalytic debromination by  $\text{TiO}_2$ . Recently, it was found that BDE209 could be an efficient reductive debrominate under visible-light irradiation ( $\geq 420\text{ nm}$ ) in the presence of various carboxylate anions [26]. This implies that some carbonylic species common in the environmental media may use to remediate PBDEs.

Pyruvic acid (2-oxopropanoic, PA) is widespread environmental carbonylic species, as ubiquitous components of surface water and the atmospheric aerosol. PA has been globally produced in the photochemical degradation of colored organic matter tinting rivers, lakes, and oceans and in the atmospheric oxidation of organic gas [27–29]. PA may undergo efficient photodecarboxylation via the excited triplet state, and excitation reaction by the  $n-\pi^*$  band in aqueous PA induces its efficient photodecarboxylation. With R-cleavage of  $3\text{PA}^*$  into geminate radical pairs, the release of  $\text{CO}_2$  follows during the subsequent reduction of PA [27,29]. These results imply that the  $n-\pi^*$  excitation of PA might induce long-range electron transfer from the promoted carbonyl chromophore into neighboring carbonyl acceptors [29]. Considering that PBDEs can undergo reductive debromination, we realize that the long-range electron transfer from  $\text{PA}^*$  might effectively reduce PBDEs to their lower bromo congeners under appropriate conditions.

In this paper, for the first time the photoreductive degradation of PBDEs by pyruvate has been investigated. BDE209 as the major product of PBDEs [1], was selected as a target PBDE. The photoreductive degradation kinetics of BDE209 has been examined. The photoreductive mechanism has been proposed on the

\* Corresponding author at: No.508 Huancheng, West Road, Shaoxing, China.  
Tel.: +86 575 8834 1521; fax: +86 0575 8834 1521.

E-mail address: [sunchunyan@usx.edu.cn](mailto:sunchunyan@usx.edu.cn) (C. Sun).

basis of experimental data. It not only provides a new method for degradation of PBDEs but also puts a new insight into the photochemistry of pyruvic acid and the fate of PBDEs in the environment due to pyruvic acid co-exist widely with the PBDEs in many environmental situations, such as the atmospheric aerosol.

## 2. Materials and methods

### 2.1. Materials

BDE209 was purchased from Aldrich Chemical Company (USA). BDE203, BDE204 and a standard solution of PBDEs (EO5103) were purchased from Cambridge Isotope Laboratories (CIL, Andover, MA). Pyruvic acid was purchased from Aldrich Chemical Company (USA).  $\text{CH}_3\text{OD}$  and  $\text{CD}_3\text{OH}$  were purchased from Cambridge Isotope Laboratories. HCl, NaOH, tetrahydrofuran, hexane, methanol were analytical reagents (Chemical Co., Shanghai). They were used without further purification. Deionized and doubly distilled water was used throughout the study.

### 2.2. Methods

#### 2.2.1. Experimental setup

BDE209 stock solution ( $1 \times 10^{-3} \text{ mol/L}$ ) in tetrahydrofuran was diluted with methanol to  $1 \times 10^{-5} \text{ mol/L}$ . 0.05 mL pyruvic acid aqueous solution ( $1 \times 10^{-2} \text{ mol/L}$ ) was added to 10 mL BDE209 methanol solution in a Pyrex vessel. Reaction solutions were magnetically stirred during the irradiation. The Pyrex vessel was purged with argon for 30 min to remove  $\text{O}_2$  and protected under argon atmosphere during the irradiation. A PLS-SXE300 Xe lamp (Beijing Trusttech Co. Ltd.) was used as the light source. To eliminate the direct photolysis of BDE209, a cutoff filter was used to cut the irradiation below 360 nm. To investigate the effect of acids/bases and  $\text{H}_2\text{O}$  on the reaction kinetics, a given amount acid/base and  $\text{H}_2\text{O}$  were added under otherwise identical conditions. At given time intervals, 1 mL aliquots were used for analysis.

#### 2.2.2. HPLC analysis

BDE209 in samples was quantified with a SHIMADZU HPLC system (LC-20AT pump and UV-vis SPD-20A detector) with a DIKMA Platisil ODS C-18 column ( $250 \times 4.6 \text{ mm}$ ,  $5 \mu\text{m}$  film thickness). The mobile phase was 2% water in acetonitrile at  $1 \text{ mL/min}$  and the detector wavelength was set at 240 nm. The quantification of BDE209 used a calibration curve with BDE209 standard.

#### 2.2.3. GC- $\mu$ ECD analysis

Products were detected by GC- $\mu$ ECD analysis. The products were extracted by hexane and the internal standards pentachlorophenol (PCP) were added to all samples before the analysis with gas chromatograph (GC) (Agilent 7890A) equipped with an electron capture detector (ECD) (Agilent Technologies Co. USA) and a programmable pressure on-column injection port and a DB-5 capillary column ( $30 \text{ m} \times 50 \mu\text{m}$ , i.d.  $\times 0.1 \mu\text{m}$  film thickness). Splitless  $10 \mu\text{L}$  injection was performed manually at  $300^\circ\text{C}$ . The carrier gas was helium at a constant flow rate of  $1.0 \text{ mL/min}$ . The oven temperature was kept at  $100^\circ\text{C}$  for 2 min, increased at  $15^\circ\text{C}/\text{min}$  to  $230^\circ\text{C}$ , then increased at  $5^\circ\text{C}/\text{min}$  to  $270^\circ\text{C}$ , and finally increased at  $10^\circ\text{C}/\text{min}$  to  $320^\circ\text{C}$  for 10 min. The standard samples of BDE203, BDE204 and PBDEs (EO5113) were used to identify the degradation products.

#### 2.2.4. UV-vis absorption spectra

UV-vis absorption spectra were conducted with  $10 \times 10 \text{ mm}$  quartz cuvettes by a Hitachi U-3010 spectrophotometer (Hitachi Co. Japan) under anoxic conditions.

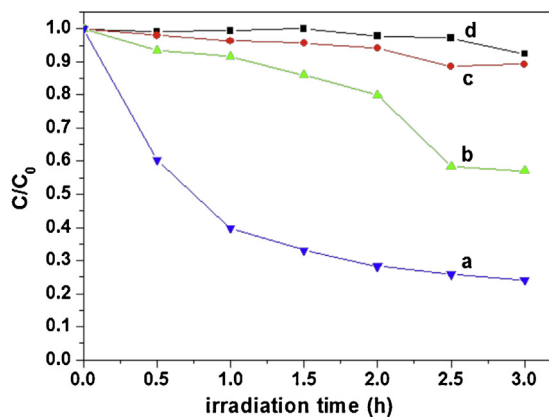


**Fig. 1.** Temporal curves of the photodegradation of BDE209 under different conditions. BDE209:  $1.0 \times 10^{-5} \text{ mol/L}$ ; sodium pyruvate:  $5.0 \times 10^{-5} \text{ mol/L}$ ; solvent: methanol/THF/ $\text{H}_2\text{O}$  (V/V: 100/1/0.5); wavelength  $>360 \text{ nm}$ ; (a) BDE209/sodium pyruvate/Ar/UV, (b) BDE209/sodium pyruvate/air/UV, (c) BDE209/sodium pyruvate/Ar/heat ( $50^\circ\text{C}$  by water bath), (d) BDE209/Ar/UV.

## 3. Results and discussion

### 3.1. Degradation kinetics

To eliminate direct photolysis of BDE209 [15,16], the irradiation below 360 nm was filtered completely. The degradation of BDE209 was scarcely observed in methanol solution without pyruvate under the UV irradiation (Fig. 1d and Fig S1). BDE209 exhibited little degradation when the reactions were carried out in the presence of pyruvate but under the air-saturated condition (Fig. 1b). However, rapid degradation of BDE209 occurred in the anoxic BDE209/sodium pyruvate solution under UV irradiation, and more than 60% of BDE209 disappeared after 1 h of irradiation (Fig. 1a). The kinetics was fitted by pseudo-first-order process, giving a rate constant of  $0.54 \pm 0.02 \text{ h}^{-1}$  ( $t_{1/2} = 0.8 \text{ h}$ ). By contrast, the reaction system containing sodium pyruvate in the dark heating in water bath under anoxic condition showed no disappearance of BDE209 (Fig. 1c). It indicated that the degradation was initiated by pyruvate-based photoreductive reaction and oxygen would decrease the degradation rate.

### 3.2. Product analysis

The product analysis by GC- $\mu$ ECD showed that the degradation of BDE209 by sodium pyruvate led to the formation of its lower brominated congeners in a stepwise way (Fig. 2). Before the irradiation, the only dominant GC peak was from BDE209, with trace nona-BDEs due to impurity. After 0.5 h, nona-BDEs appeared as main intermediates. Nona-BDEs and octa-BDEs appeared as main intermediates, concomitantly with the significant decrease of BDE209 after 1 h. After irradiation of 14 h, the octa-BDEs and hepta-BDEs were measured as the dominant intermediates. All PBDE congeners with more than octa-BDEs vanished, and transformed to hexa-BDEs/penta-BDEs at further prolonged irradiation.

The degradation products were identified with chemical standards (Fig. 3). The first step was the loss of one bromine atom to form three nona-BDEs. After 0.5 h, all nona-BDEs appeared, which was identified to be BDE208, 207, and 206, respectively, according to their well-established GC elution orders [30,31]. There were five octa-BDEs observed after 2 h. BDE203 and BDE204 were identified by the chemical standards. The peak with a retention time slightly longer than that of BDE203 was BDE196, according to the relative retention times and the orders of GC elution obtained from the literatures [23,30,31]. Six hepta-BDEs were detected after 14 h of irradiation. BDE183, BDE181 and BDE190 were identified

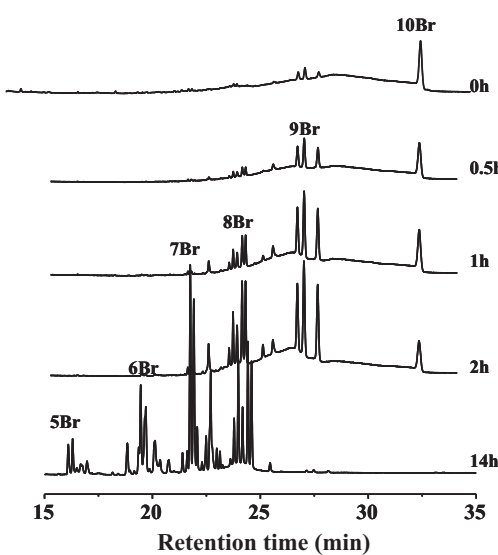


**Fig. 2.** GC- $\mu$ ECD chromatograms of degradation products of BDE209 in methanol at different irradiation times. Reaction conditions: BDE209:  $1.0 \times 10^{-5}$  mol/L; sodium pyruvate:  $5.0 \times 10^{-5}$  mol/L, wavelength  $>360$  nm, solvent: methanol/THF/H<sub>2</sub>O (V/V: 100/1/0.5).

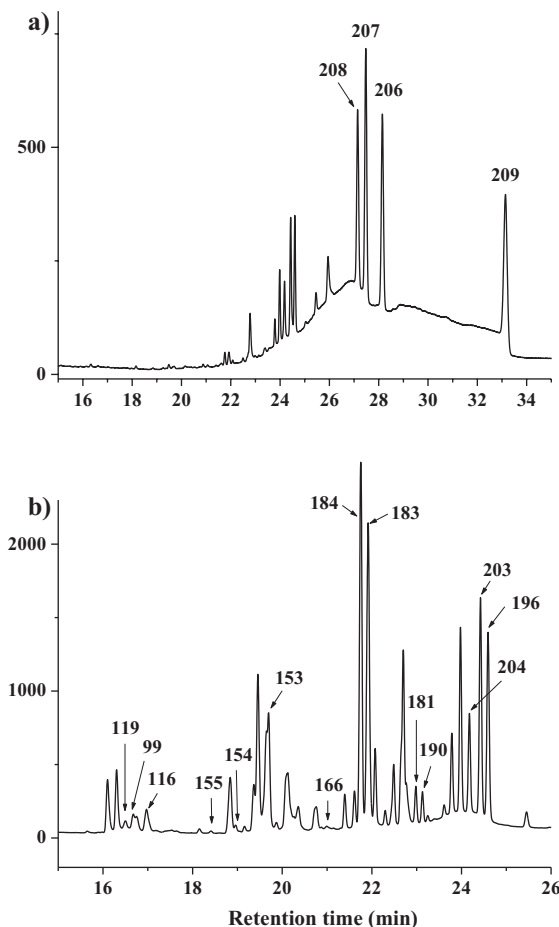


**Fig. 3.** Products identification with GC- $\mu$ ECD chromatograms by the retention time of standard samples. (a) 1 h, (b) 14 h. Reaction conditions: BDE209:  $1.0 \times 10^{-5}$  mol/L; sodium pyruvate:  $5.0 \times 10^{-5}$  mol/L wavelength  $>360$  nm, solvent: methanol/THF/H<sub>2</sub>O (V/V: 100/1/0.5).

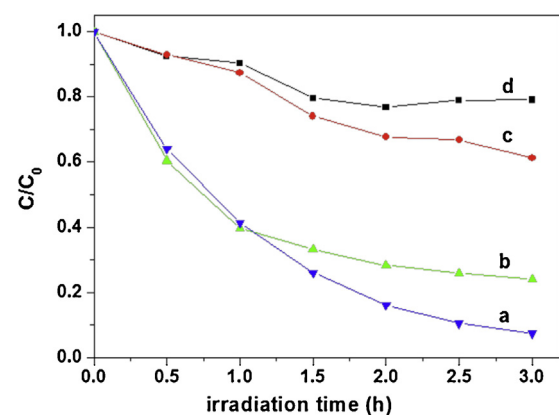


**Fig. 4.** Effect of acid/base on the photoreductive degradation of BDE209 by pyruvate in CH<sub>3</sub>OH under UV irradiation. BDE209,  $1.0 \times 10^{-5}$  mol/L; sodium pyruvate:  $5.0 \times 10^{-5}$  mol/L, solvent: methanol/THF/H<sub>2</sub>O (V/V: 100/1/0.5); (a) 0.01 M NaOH, (b) no HCl/NaOH, (c) 0.06 M HCl, (d) 0.12 M HCl.

with the chemical standards. The peak, whose retention time was slightly shorter than that of BDE183, could be assigned as BDE184 based on the retention time of literature [30]. Four hexa-BDEs peaks were identified to be BDE155, BDE154, BDE153 and BDE166, respectively, with the chemical standards. Three penta-BDEs were identified and they were BDE119, BDE99 and BDE116, respectively.

Among all intermediates, the products of first debromination step (nona-BDEs) provide direct information of the debromination pathway of BDE209. All the three nona-BDE intermediates were identified during the photocatalytic reductive reaction. They were BDE206, BDE207, and BDE208, corresponding to *ortho*-, *meta*-, and *para*-debrominated intermediates of BDE209, respectively. Their relative peak areas were in the orders for BDE207 > BDE208 > BDE206 (1:0.87:0.72) after 1 h. It indicated that the debromination by pyruvate showed unspicuous position-selective property, which was different from our previous studies in photocatalytic TiO<sub>2</sub> system [23]. In TiO<sub>2</sub> system, *ortho*-debromination was much easier than those from others, and debromination from the *para* position was the most unfavorable pathway with peak areas in the orders for BDE206 > BDE207 > BDE208 (1:0.25:0.16). This showed that the debromination pattern of BDE209 varied greatly in the different reducing system. Identification as other lower brominated intermediate showed that the *meta*-debromination was slightly easier than those from other positions, and the debromination mainly showed no obvious position-selective in pyruvate system.

### 3.3. Effect of acid and base

The degradation experiments were performed under the addition acid and base into the solution. As illustrated in Fig. 4, when HCl added the reaction suppressed markedly and addition of NaOH accelerated the degradation of BDE209. It is well known that pyruvic acid appears ionization balance in the solution due to weak acid. The concentration of pyruvate anions changed with the addition of acid and base in the solution. Accordingly, the concentration of pyruvate anions should be much lower in the solution after addition of HCl and higher in the solution after addition of NaOH. It implied that the photochemical reactivity was closely related to the concentration of pyruvate anions. In other words, pyruvate anion was the key factor in the reaction for degradation of BDE209.

### 3.4. Effect of H<sub>2</sub>O

To investigate the effect of H<sub>2</sub>O in the photoreductive degradation of PBDEs by pyruvate, the reactions were further carried out

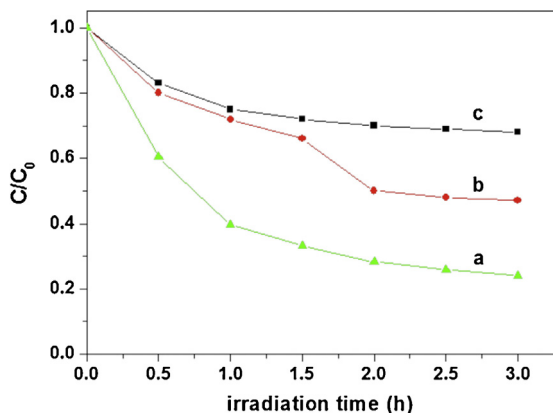


**Fig. 5.** Temporal curves of the photodegradation of BDE209 under different conditions. BDE209:  $1.0 \times 10^{-5}$  mol/L, sodium pyruvate:  $5.0 \times 10^{-5}$  mol/L, wavelength  $>360$  nm, purged with argon. (a) methanol/THF/H<sub>2</sub>O (V/V: 100/1/0.5), (b) methanol/THF/H<sub>2</sub>O (V/V: 100/1/1), (c) methanol/THF/H<sub>2</sub>O (V/V: 100/1/2).

with different ratios of H<sub>2</sub>O. As seen from Fig. 5, the rate of degradation was depressed with the ratio of H<sub>2</sub>O increasing. When the ratio of H<sub>2</sub>O was 0.5%, about 60% of BDE209 disappeared after 1 h. Nevertheless, the rate of degradation was depressed on some extent when the ratio of H<sub>2</sub>O was 1%. The rate of BDE209 degradation was markedly depressed in menthol with 2% of H<sub>2</sub>O. The results indicated that the degradation of BDE209 would markedly be suppressed in the presence of water. BDE209 is strongly hydrophobic, but pyruvate is quite hydrophilic. The pyruvate would be preferentially dissolved in water, which would block the interaction between pyruvate and BDE209, and further inhibit the electron transfer from pyruvate in its excited state to BDE209 molecular. Thus water may produce adverse effect on the degradation of BDE209 by pyruvate.

### 3.5. UV-vis absorption spectra

The measurement of UV-vis absorption spectra indicated that neither sodium pyruvate nor BDE209 had absorption beyond 360 nm (Fig. 6 spectra a and b, respectively), which is consistent with the above observation that BDE209 alone is stable under irradiation beyond 360 nm (Fig. 1d). However, a new absorption band appeared in the pyruvate/BDE209 solution in the wavelength region of 350–600 nm (Fig. 6 spectra c). It indicated that the enhanced absorption led to pyruvate excitation by irradiation (wavelength  $>360$  nm) and at last resulted in the debromination

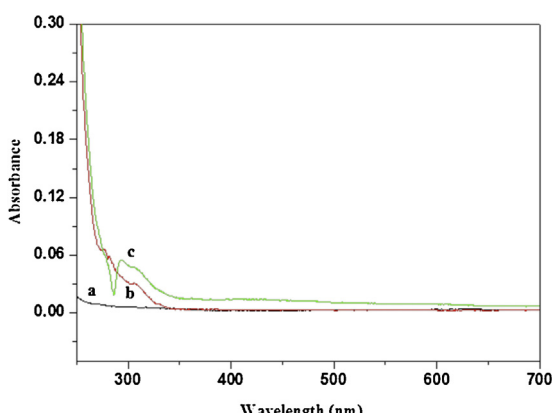


**Fig. 6.** UV-vis absorption spectra in CH<sub>3</sub>OH solution. (a): sodium pyruvate, (b): BDE209, (c): BDE209/sodium pyruvate. BDE209:  $1.0 \times 10^{-5}$  mol/L, sodium pyruvate:  $5.0 \times 10^{-5}$  mol/L. Solvent: methanol/THF/H<sub>2</sub>O (V/V: 100/1/0.5).

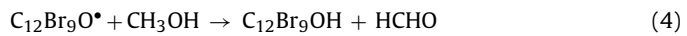
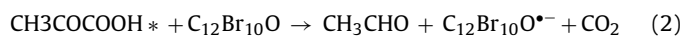
of BDE209. The attempt to estimate the quantum efficiency of the photochemical reaction was unsuccessful because the enhanced absorption was rather weak. On the other hand, the weak absorption but rapid photochemical reaction implied that the photoefficiency of the halogen-bond system might be quite high.

### 3.6. Kinetic isotope effect

Kinetic isotope effect (KIE) is the ratio of the rate constants of a reactant, which has an isotopic substitution. KIE will help understand the mechanisms of a reaction and indicate the rate-determining step in the degradation reaction. KIE basically owns two types [32]: Primary KIE and Secondary KIE. Primary KIE occurs when substitution is done at the bond which reacts. Secondary KIE happens when the substitution is at a bond other than the one which reacts. In the degradation reaction, BDE209 was firstly reduced by getting electron from pyruvate to generate BDE209<sup>•-</sup> radical and then followed by abstracting hydrogen from solvent. So the KIE experiments may reveal more information about the mechanism of degradation BDE209 by pyruvate. We performed degradation experiments under the same condition with CH<sub>3</sub>OD and CD<sub>3</sub>OH as solvent respectively, replacing of CH<sub>3</sub>OH. As illustrated in Fig. S2, the results showed that the degradation rate of BDE209 was un conspicuous varied by deuterium substituted solvent. The KIE was  $1.01 \pm 0.1$  for CH<sub>3</sub>OD and  $1.03 \pm 0.2$  for CD<sub>3</sub>OH. There was no obvious KIE in the reaction. The results indicated that abstracting hydrogen from solvent is not the rate determining step in the degradation reaction of BDE209 by pyruvate.

### 3.7. A possible reaction mechanism

Based on the above experiments, a possible reaction mechanism has been proposed. Halogen atoms in aromatic compounds are known to possess positive surface region along their covalent bond, which makes the halogen atom easy to interact with the electron donor [26]. Such noncovalent interactions are referred to halogen bonds by analogy with the better-known hydrogen bonds. The halogen-bond interaction between the bromine atom of BDE209 and the O atom of pyruvate anion induced the stronger absorption than BDE209 and pyruvate alone respectively. The enhanced absorption led to pyruvate excitation by irradiation (wavelength  $>360$  nm) (Eq. (1)). Then the n-π\* excitation of PA ion [29] induced long-range electron transfer from the promoted carbonyl chromophore into neighboring BDE209 molecular. Subsequently, PA lost electron and changed to CO<sub>2</sub> and CH<sub>3</sub>CHO [28,29] (Eq. (2)). BDE209 obtained electron and formed C<sub>12</sub>Br<sub>9</sub>O<sup>•-</sup> and Br<sup>-</sup> (Eq. (3)). The C<sub>12</sub>Br<sub>9</sub>O<sup>•-</sup> radical abstracted hydrogen atom from methanol and yielded lower bromo congeners C<sub>12</sub>Br<sub>9</sub>OH and CH<sub>3</sub>OH transformed to HCHO with losing hydrogen atom (Eq. (4)).



The theoretical calculations indicated that the strength of halogen bond greatly depended on the existence state of pyruvate [26]. The strength of the halogen bond became stronger with the concentration of pyruvate anion increasing. Thus the addition of HCl (NaOH) suppressed (accelerated) the degradation of BDE209 due to the concentration of pyruvate anion changing.

## 4. Conclusions

BDE209 showed efficient reductive debromination by pyruvate under UV irradiation (>360 nm). The photoreductive degradation kinetics of BDE209 was further investigated under different reaction conditions. It showed that addition of HCl depressed the degradation of BDE209 and addition of NaOH accelerated the degradation. In addition, degradation of BDE209 would markedly be suppressed in water because the electron transferred from PA to BDE209 would be held back due to strong hydrophobic ability of BDE209. The debromination reactions occurred in a stepwise process, producing a series of lower brominated congeners. The debromination showed un conspicuous position-selective property. The possible photoreductive mechanism was proposed by kinetic isotope effect (KIE) and UV-vis absorption spectra. The halogen–bond interaction between the bromine atom of BDE209 and the O atom of pyruvate anion induced the stronger absorption, which led to pyruvate excitation by irradiation (wavelength >360 nm) and debromination of BDE209 by pyruvate. The KIE experiment showed that abstracting hydrogen from solvent was not the rate determining step in the degradation of BDE209 by pyruvate.

Our study on the photochemical debromination of PBDEs by pyruvate under irradiation may present some environmental implication. Considering that pyruvate co-exists widely with PBDEs in many environmental situations, such as atmospheric aerosol, photochemical debromination of PBDEs in the presence of pyruvate under irradiation may represent an important pathway for the transformation of the PBDEs. Their contributions to the transformation of PBDEs in the environment should be taken into account in evaluating the ecological effects and the environmental fate of PBDEs.

## Acknowledgments

The generous financial support by the National Science Foundation of China (Nos. 21107073 and 21143003) and the Natural Science Foundation of Zhejiang province (Nos. Y5110347, 5100229) and the new-shoot Talents Program of Zhejiang province (2012R426014).

## Appendix A. Supplementary data

Supplementary data associated with this article can be found, in the online version, at <http://dx.doi.org/10.1016/j.cattod.2014.01.002>.

## References

- [1] L.S. Brinbaum, D.F. Staskal, *Environ. Health Perspect.* 112 (2004) 9–17.
- [2] B. Mai, S. Chen, X. Luo, L. Chen, Q. Yang, G. Sheng, P. Peng, J. Fu, E. Zeng, *Environ. Sci. Technol.* 39 (2005) 3521–3527.
- [3] C.A. de Wit, *Chemosphere* 46 (2002) 583–624.
- [4] A. Kierkegaard, L. Balk, U. Tjarnlund, C.A. de Wit, B. Jansson, *Environ. Sci. Technol.* 33 (1999) 1612–1617.
- [5] H.M. Stapleton, B. Brazil, R.D. Holbrook, C.L. Mitchelmore, R. Benedict, A. Konstantinov, D. Potter, *Environ. Sci. Technol.* 40 (2006) 4653–4658.
- [6] N. Wu, T. Herrmann, O. Paepke, J. Tickner, R. Hale, E. Harvey, M. La Guardia, M.D. McClean, T.F. Webster, *Environ. Sci. Technol.* 47 (2007) 1584–1589.
- [7] P.O. Darnerud, S. Atuma, M. Aune, S. Cnattingius, M.L. Wernroth, A. Wicklund Glynn, *Organohalogen Compd.* 35 (1998) 411–414.
- [8] M.G. Ikonomou, S. Rayne, R.F. Addison, M. Alaee, P. Arias, S.A. Bergman, *Environ. Int.* 29 (2003) 683–689.
- [9] C.A. de Wit, M. AlapA., D.C.G. Muir, *Chemosphere* 64 (2006) 209–233.
- [10] P.O. Darnerud, G.S. Eriksen, T. Jóhannesson, P.B. Larsen, M. Viluksela, *Environ. Health Perspect.* 109 (2001) 49–68.
- [11] I.A.T.M. Meerts, R.J. Letcher, S. Hoving, G. Marsh, A. Bergman, J.G. Lemman, B. van der Burg, A. Brouwer, *Environ. Health Perspect.* 109 (2001) 399–407.
- [12] M.Y. Ahn, T.R. Filley, C.T. Jafvert, L. Nies, I. Hua, J. Bezares-Cruz, *Environ. Sci. Technol.* 40 (2006) 215–220.
- [13] J. Bezares-ruz, C.T. Jafvert, I. Hua, *Environ. Sci. Technol.* 38 (2004) 4149–4156.
- [14] I. Watanabe, R. Tatsukawa, *Environ. Contam. Toxicol.* 39 (1987) 953–959.
- [15] G. Söderström, U. Sellström, A.C. de Wit, M. Tysklin, *Environ. Sci. Technol.* 38 (2004) 127–132.
- [16] J. Eriksson, N. Green, G. Marsh, Å. Bergman, *Environ. Sci. Technol.* 38 (2004) 3119–3125.
- [17] A.C. Gerecke, P.C. Hartmann, N.V. Heeb, H.E. Kohler, W. Giger, P. Schmid, M. Zennegg, M. Kohler, *Environ. Sci. Technol.* 39 (2005) 1078–1083.
- [18] Y.S. Keum, Q.X. Li, *Environ. Sci. Technol.* 39 (2005) 2280–2286.
- [19] A. Li, C. Tai, Z.S. Zhao, Y.W. Wang, Q.H. Zhang, G.B. Jiang, J.T. Hu, *Environ. Sci. Technol.* 41 (2007) 6841–6846.
- [20] Y. Zhuang, S. Ahn, R. Luthy, *Environ. Sci. Technol.* 44 (2010) 8236–8242.
- [21] Y. Zhuang, S. Ahn, A.L. Seyfferth, Y. Masue-Slowey, S. Fendorf, R.G. Luthy, *Environ. Sci. Technol.* 45 (2011) 4896–4903.
- [22] C.Y. Sun, D. Zhao, C.C. Chen, W.H. Ma, J.C. Zhao, *Environ. Sci. Technol.* 43 (2009) 157–162.
- [23] C.Y. Sun, J.C. Zhao, H.W. Ji, W.H. Ma, C.C. Chen, *Chemosphere* 89 (2012) 420–425.
- [24] C.Y. Sun, C.C. Chen, W.H. Ma, J.C. Zhao, *Sci. China Chem.* 55 (2012) 2532–2536.
- [25] A. Huang, N. Wang, M. Lei, L.H. Zhu, Y.Y. Zhang, Z.F. Lin, D.Q. Yin, H.Q. Tang, *Environ. Sci. Technol.* 47 (2013) 518–525.
- [26] C.Y. Sun, W. Chang, W.H. Ma, C.C. Chen, J.C. Zhao, *Environ. Sci. Technol.* 47 (2013) 2370–2377.
- [27] S. Yamamoto, R.A. Back, Can, *J. Chem.* 63 (1985) 549–554.
- [28] S. Dhanya, D.K. Maity, H.P. Upadhyaya, A. Kumar, P.D. Naik, *J. Chem. Phys.* 118 (2003) 10093–10100.
- [29] M.I. Guzmán, A.J. Colussi, M.R. Hoffmann, *J. Phys. Chem. A* 110 (2006) 931–935.
- [30] P. Korttär, A. Covaci, J. Boer, A. Gelbin, U.A.T. Brinkman, *J. Chromatogr. A* 1065 (2005) 239–249.
- [31] Y.W. Wang, A. Li, H.X. Liu, Q.H. Zhang, W.P. Ma, W.L. Song, G.B. Jiang, *J. Chromatogr. A* 1103 (2006) 314–328.
- [32] G. Parkin, *Acc. Chem. Res.* 42 (2009) 315–325.